

# Tungstate versus Molybdate Adsorption on Oxidic Surfaces: A Chemical Approach

Marcel J. Vissenberg,<sup>†</sup> Lieke J. M. Joosten,<sup>†</sup> Myriam M. E. H. Heffels,<sup>†</sup>  
Arend Jan van Welsenes,<sup>‡</sup> V. H. J. (San) de Beer,<sup>\*,†</sup> Rutger A. van Santen,<sup>†</sup> and  
J. A. Rob van Veen<sup>†</sup>

Schuit Institute of Catalysis, Eindhoven University of Technology, P.O. Box 513,  
5600 MB Eindhoven, The Netherlands Shell Research and Technology Centre Amsterdam,  
P.O. Box 38000, 1030 BN Amsterdam, The Netherlands

Received: October 20, 1999; In Final Form: June 1, 2000

The differences between the chemistry of tungstate adsorption on oxidic supports and that of molybdate (viz.  $\gamma$ - $\text{Al}_2\text{O}_3$ ,  $\text{TiO}_2$  and amorphous silica alumina (ASA)) were studied by measuring equilibrium adsorption isotherms at various conditions (pH, (co)-adsorption of tungstate and molybdate), by determining which part was reversibly adsorbed, and by structurally characterizing them using FTIR and Raman spectroscopy. It can be concluded that most of the tungstate reacts irreversibly with acidic and neutral OH groups, and the other part adsorbs reversibly by electrostatic interactions with protonated OH groups, whereas molybdate irreversibly reacts in a reaction with the basic OH groups. However, as soon as these groups are protonated, molybdate also starts to reversibly adsorb by electrostatic interactions. In addition, molybdate adsorbs on coordinatively unsaturated sites whereas tungstate does not.

## Introduction

The interaction between transition metal oxides and refractory oxide support materials (such as  $\text{Al}_2\text{O}_3$ ,  $\text{TiO}_2$ , or amorphous silica alumina (ASA)) is an important parameter in the process of catalyst preparation. In the case of hydrotreating catalysts, this interaction determines the sulfidability of the metal (oxides), the dispersion, the morphology and the electronic properties of the metal (sulfides). Equilibrium adsorption provides information about the manner in which tungstate and molybdate interact with the support. Unfortunately, most adsorption studies are based on pure modeling rather than chemical or spectroscopic characterization.<sup>1–8</sup> Only in a few studies<sup>9–15</sup> are any attempts made to explain the adsorption isotherms using a chemical model in combination with checking by spectroscopic characterization. For adsorption, the presence of different sites on a surface is important. Depending on the pH and type of support, coordinatively unsaturated sites (CUS), basic, neutral, and acidic OH groups (whether protonated) can be present. These different adsorption sites and possible molybdate adsorption modes are shown in Figure 1.

Lycourghiotis's group performed an extensive study on the modeling of tungstate and molybdate adsorption isotherms.<sup>1–5</sup> They assumed that tungstate and molybdate adsorb on the same sites. The adsorption step, depending on the pH, was thought either to consist of a condensation reaction between tungstate or molybdate and the neutral surface OH (at pH 8.5–6) or to consist of an electrostatic interaction as a result of surface charging by protonation of hydroxyl groups (at pH < 5).

Mulcahy et al.<sup>6</sup> concluded that tungstate and molybdate adsorb on two types of surface sites producing loosely and tightly bound surface species, both of which are polymeric in nature. Two types of basic alumina hydroxyl groups were

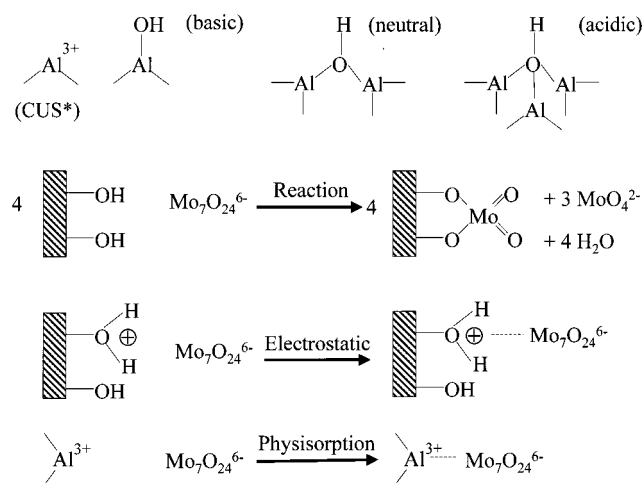


**Figure 1.** Simplified scheme of adsorption sites and possible molybdate adsorption modes. \*Coordinatively Unsaturated Sites.

suggested to be responsible for the differently bounded species. So, tungstate as well as molybdate adsorbs on the basic OH sites.

Van Veen et al.<sup>9–11</sup> concluded, based on FTIR, Raman Spectroscopy, TPR, and EXAFS, that molybdate adsorption on alumina cannot be explained in terms of electrostatic bonding to protonated surface hydroxyls but can be rationalized by assuming a reaction between molybdate and basic surface OH groups, leading to the decomposition of the adsorbing molecule or ion together with physisorption on coordinatively unsaturated sites (CUS).

A study was carried out to describe the tungstate adsorption and, thus, to determine whether tungstate and molybdate adsorb according to the same mechanism. This study was focused on chemical and spectroscopic characterization. Adsorption isotherms of tungstate and molybdate on different supports ( $\text{Al}_2\text{O}_3$ ,  $\text{TiO}_2$ , and ASA) and at two pH values (near neutral and pH

<sup>†</sup> Schuit Institute of Catalysis.

<sup>‡</sup> Shell Research and Technology Centre Amsterdam.

**TABLE 1: An Overview of the Equilibrium Adsorption Measurements**

experiment	Al <sub>2</sub> O <sub>3</sub>	TiO <sub>2</sub>	ASA (17:83) <sup>a</sup>
Tungstate adsorption			
pH near neutral	X	X	X
SO <sub>4</sub> <sup>2-</sup> exchange	X	X	X
pH 1.9	X	X	X
SO <sub>4</sub> <sup>2-</sup> exchange	X		
Molybdate adsorption			
pH near neutral	X	X	X
SO <sub>4</sub> <sup>2-</sup> exchange	X	X	X
pH 1.9	X	X	X
SO <sub>4</sub> <sup>2-</sup> exchange	X		
Tungstate and Molybdate coadsorption			
pH near neutral	X	X	

<sup>a</sup> (wt% Al<sub>2</sub>O<sub>3</sub>: wt% SiO<sub>2</sub>)

1.9) were measured. Eventually, competition between tungstate and molybdate for adsorption sites was studied by coadsorption from solutions containing both tungstate and molybdate. By contacting a SO<sub>4</sub><sup>2-</sup> solution with tungstate or molybdate adsorbed on Al<sub>2</sub>O<sub>3</sub>, it was determined which fraction of the tungstate or molybdate could be exchanged for SO<sub>4</sub><sup>2-</sup> anions. Some structural information was obtained by FTIR and Raman spectroscopy.

### Experimental Section

All adsorption experiments carried out are listed in Table 1. For each point of the adsorption isotherm, 4 g of support was calcined by heating 1 h from 298 to 673 K and maintaining it for 2 h at this temperature. Extrudates of  $\gamma$ -Al<sub>2</sub>O<sub>3</sub> (Ketjen, CK300 001–1.5E/3E 0.1, BET surface area 260 m<sup>2</sup>/g) or TiO<sub>2</sub> (Degussa P25, BET surface area 50 m<sup>2</sup>/g, anatase: rutile 75:25) were used. For comparison, a second  $\gamma$ -Al<sub>2</sub>O<sub>3</sub> batch (Ketjen, CK300, BET surface area 190 m<sup>2</sup>/g) was used. This latter support will be denoted as Al<sub>2</sub>O<sub>3</sub>(surface area 190 m<sup>2</sup>/g). ASA, having a BET surface area of about 360 m<sup>2</sup>/g, was prepared via a co-gelling reaction<sup>16</sup> and contained 17 wt % Al<sub>2</sub>O<sub>3</sub> and 83 wt % SiO<sub>2</sub> (called ASA(17:83)).

Aqueous solutions with increasing concentration of Mo and/or W were obtained by dissolving ammonium heptamolybdate (AHM) and/or ammonium metatungstate (AMT) in water. The pH of these solutions will be referred to as pH at near neutral conditions. When necessary, the pH of the solution was adjusted to 1.9 with HNO<sub>3</sub>. It was checked by Raman and XRD that no heteropolyanions were formed as reported by Carrier et al.<sup>17,18</sup> Indeed, in line with the findings of Regalbuto et al.,<sup>19</sup> we do not think that Al dissolution is interfering with our adsorption experiments. Subsequently, the support was contacted with 100 mL of these solutions and the solid–liquid mixture was shaken occasionally. The standard adsorption time was 5 days. In the case of Al<sub>2</sub>O<sub>3</sub>, the metal uptake was determined by AAS (relative error  $\pm$  2%) after destruction of the support with a mixture of HF:HNO<sub>3</sub>:H<sub>2</sub>O (1:1:1). The metal uptake on TiO<sub>2</sub> was analyzed with XRF.

SO<sub>4</sub><sup>2-</sup> exchange experiments were carried out by contacting adsorbed tungstate or molybdate on Al<sub>2</sub>O<sub>3</sub> (filtered, nondried samples) with 100 mL of 0.1 M (NH<sub>4</sub>)<sub>2</sub>SO<sub>4</sub> for 4 h with continuous shaking. The remaining metal on Al<sub>2</sub>O<sub>3</sub> was measured by AAS.

NO<sub>3</sub><sup>-</sup> adsorption was used to get an impression of the surface charging of Al<sub>2</sub>O<sub>3</sub> and TiO<sub>2</sub> at different pH values. Calcined Al<sub>2</sub>O<sub>3</sub> or TiO<sub>2</sub> extrudates were contacted with a 0.1 M KNO<sub>3</sub>

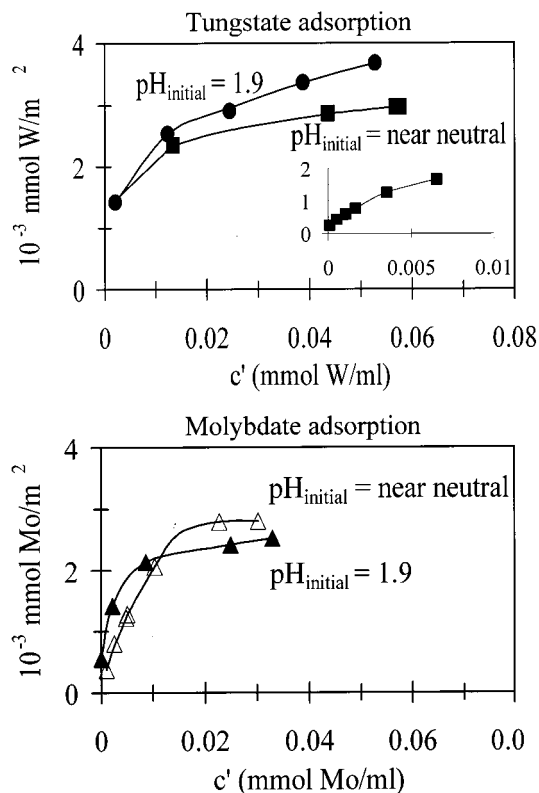


**Figure 2.** Tungstate/Al<sub>2</sub>O<sub>3</sub> and molybdate/Al<sub>2</sub>O<sub>3</sub> adsorption isotherms at pH<sub>initial</sub> near neutral and pH<sub>initial</sub> 1.9. The inset shows tungstate/Al<sub>2</sub>O<sub>3</sub> at very low concentrations at pH<sub>initial</sub> near neutral.

solution for 4 h with continuous shaking. The pH of the solutions was adjusted with HNO<sub>3</sub> to 1, 2, 3.5, 4.5, and 6. FTIR was used for quantitative analysis by using a sample impregnated with KNO<sub>3</sub> [0.066 mmol NO<sub>3</sub>/g Al<sub>2</sub>O<sub>3</sub> (TiO<sub>2</sub>)] as a reference. FTIR measurements were carried out on a Shimadzu FTIR-8300. Before measuring the NO<sub>3</sub><sup>-</sup> adsorption samples, they were grounded, mixed with KBr, and pressed into a pellet. Mixing with KBr was done in two steps to obtain a 3 mg sample in a pellet.

To obtain information on the OH group population FTIR spectroscopy of self-supported wafers was utilized (a single-beam Mattson FTIR instrument). Before a spectrum was recorded, the sample was evacuated at  $T > 723$ , to obtain well-resolved spectra.

Raman spectra were recorded using a Spex Ramalog spectrometer equipped with a microscope stage and an optical multichannel analyzer (OMA). Excitation was by an argon+ laser, wavelength 514.5 nm.

### Results and Discussion

Tungstate and molybdate may, in principle, adsorb at several surface sites of the support, i.e., basic, neutral, or acidic OH groups; protonated OH groups; and CUS sites. This is schematically represented in a simplified form in Figure 1.<sup>20,21</sup> To discriminate between tungstate adsorption on nonprotonated or protonated OH groups, at low pH the basic OH will be protonated,<sup>9,22</sup> the adsorption isotherms of tungstate at two different initial pH values were measured. The effect of the pH for adsorption isotherms on Al<sub>2</sub>O<sub>3</sub> is illustrated in Figure 2.

In contrast to what is claimed by Pizzio et al.,<sup>7</sup> no indications for a sigmoid adsorption curve are found (see inset Figure 2). Furthermore, it can be seen that by lowering the pH and thus protonating the OH groups, the amount of adsorbed tungstate

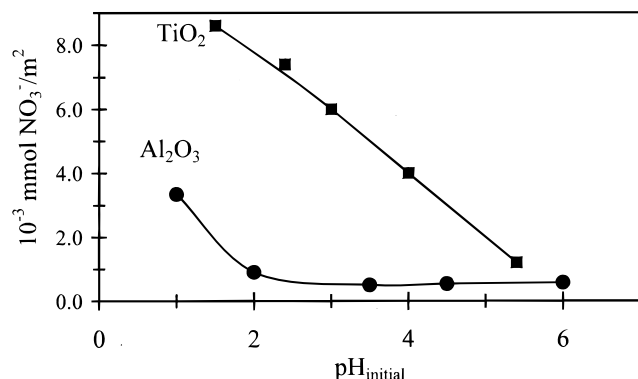


**Figure 3.** NO<sub>3</sub><sup>-</sup> adsorption on Al<sub>2</sub>O<sub>3</sub> and TiO<sub>2</sub> at various pH<sub>initial</sub> values.

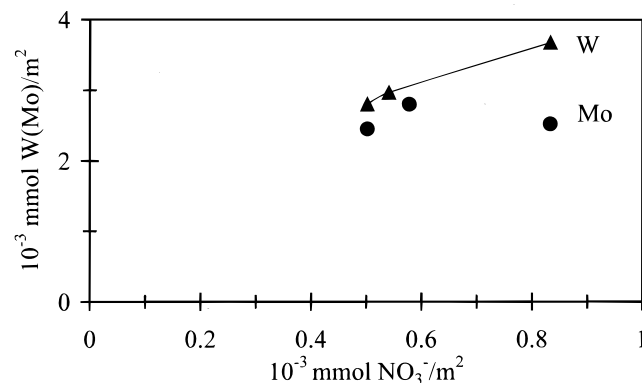


**Figure 4.** W/Al<sub>2</sub>O<sub>3</sub> and Mo/Al<sub>2</sub>O<sub>3</sub> uptake versus NO<sub>3</sub><sup>-</sup>/Al<sub>2</sub>O<sub>3</sub> uptake at corresponding pH<sub>initial</sub> values. The pH corresponding to the data points from left to right decreases from about 5 to approximately 2.

increases. This indicates that protonated OH groups play a role in tungstate adsorption. To demonstrate the existence of this type of surface sites, we studied adsorption of NO<sub>3</sub><sup>-</sup>, which will only electrostatically adsorb on protonated OH groups. Figure 3 shows the amount of adsorbed NO<sub>3</sub><sup>-</sup> as a function of the pH. Obviously, the adsorption of NO<sub>3</sub><sup>-</sup> increases at lower pH. It follows from this figure that the protonation of the Al<sub>2</sub>O<sub>3</sub> surface OH groups starts around pH 1.9. Figure 4 shows the equilibrium amounts of tungstate and NO<sub>3</sub><sup>-</sup> adsorbed at different pH values. It becomes apparent that one increases with the other. This suggests that tungstate at least partially adsorbs on the same sites as NO<sub>3</sub><sup>-</sup>. Therefore, like NO<sub>3</sub><sup>-</sup>, tungstate also adsorbs electrostatically on protonated OH groups, as expected. (It cannot be excluded that the acidic groups play a role, but this will not depend on the pH. It is conceivable that they are responsible for the adsorption taking place at higher pH values.)

By using an Al<sub>2</sub>O<sub>3</sub> batch having a surface area of 190 m<sup>2</sup>/g (older CK300 ex Ketjen) instead of 260 m<sup>2</sup>/g, another dependency between amount of NO<sub>3</sub><sup>-</sup> adsorbed and pH is found (Figure 5). In this case, the protonation starts already at higher pH. However, for this Al<sub>2</sub>O<sub>3</sub> (surface area 190 m<sup>2</sup>/g), it is found that the dependency between pH and tungstate adsorption was similar to the dependency between pH and NO<sub>3</sub><sup>-</sup>. The different pH behavior of the two Al<sub>2</sub>O<sub>3</sub> batches clearly demonstrates that the support is an important parameter in adsorption experiments, most likely due to a varying ratio between the various types of adsorption sites.

To check whether the tungstate adsorption is completely electrostatic and thus reversible, the exchange of adsorbed tungstate with SO<sub>4</sub><sup>2-</sup> was studied. Figure 6 shows the amount of adsorbed tungstate before and after exchange with SO<sub>4</sub><sup>2-</sup>. Tungstate is partly exchanged for SO<sub>4</sub><sup>2-</sup> after adsorption at pH<sub>initial</sub> is near neutral as well as after adsorption at pH<sub>initial</sub> is

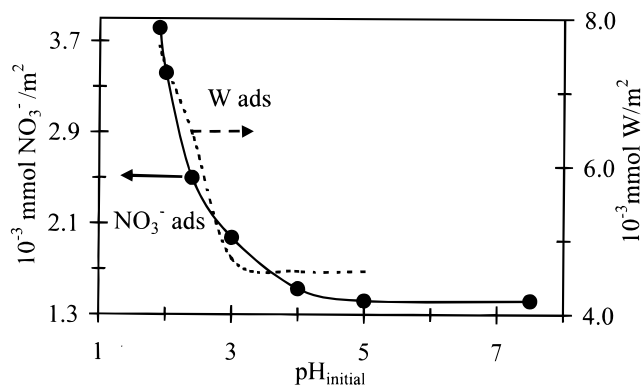


**Figure 5.** NO<sub>3</sub><sup>-</sup> and tungstate adsorption on the second batch Al<sub>2</sub>O<sub>3</sub> CK300 (surface area 190 m<sup>2</sup>/g) as a function of the pH<sub>initial</sub>.

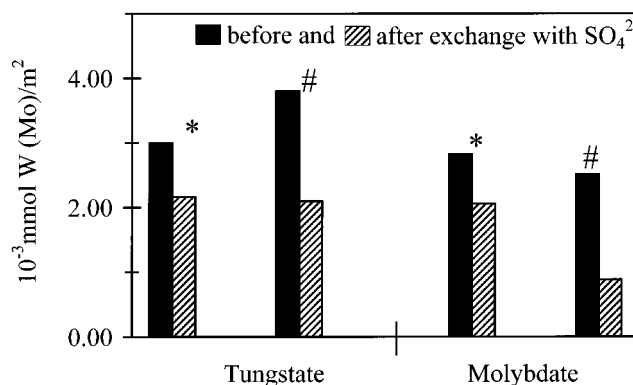


**Figure 6.** Tungstate/Al<sub>2</sub>O<sub>3</sub> and molybdate/Al<sub>2</sub>O<sub>3</sub> adsorbed before and after exchange with SO<sub>4</sub><sup>2-</sup> at (\*) pH<sub>initial</sub> near neutral and (#) pH<sub>initial</sub> 1.9.

1.9, albeit that in the latter case, the fraction of tungstate exchanged is largest. The amount of tungstate that remained on the support is independent of the pH used at the start of AMT adsorption.

We take it that this part is not adsorbed electrostatically and the question is now, which surface site is involved then. It is known that the intensity of the Raman signal depends on the strength of the tungstate support interaction.<sup>23–25</sup> The absence of a Raman signal at about 940 cm<sup>-1</sup> at low tungstate loading (Figure 7) indicates that tungstate is strongly interacting with the Al<sub>2</sub>O<sub>3</sub> surface suggesting that exchange for SO<sub>4</sub><sup>2-</sup> will be difficult. On the other hand, the appearance of a Raman signal at higher tungstate loading suggests that a part of the tungstate is bonded more loosely. This is in line with the observation that only part of tungstate can be exchanged for SO<sub>4</sub><sup>2-</sup>. So, one part of the tungstate adsorbs electrostatically on protonated OH groups, whereas another part adsorbs irreversibly in another way.

The sites, in principle, available for this irreversible adsorption are nonprotonated OH groups (basic, neutral, and acidic) and CUS sites. IR spectra (Figure 8) nicely illustrate that under near-neutral conditions, tungstate prefers adsorption on the neutral and acidic OH groups above adsorption on the basic ones. Only at higher tungstate concentration, the intensity of the IR band due to the basic OH groups starts to decrease as result of tungstate adsorption while at lower tungstate concentrations the intensity of the IR band caused by the neutral and acidic OH groups already decreases.

This is in line with the results obtained from tungstate adsorption on an Al<sub>2</sub>O<sub>3</sub> surface modified with MoO<sub>2</sub>(acac)<sub>2</sub>. It is known<sup>12</sup> that this acac (acetylacetonate) complex reacts with the basic OH groups and that the formed H-acac adsorbs on

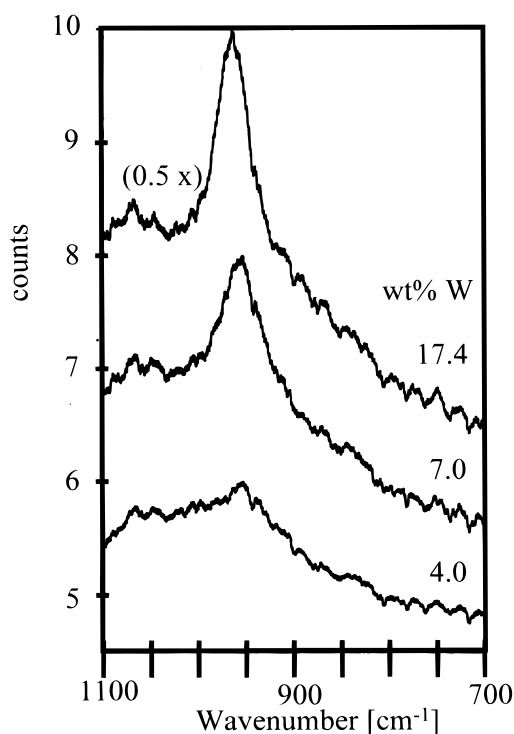


**Figure 7.** Raman spectra of tungstate/ $\text{Al}_2\text{O}_3$  as a function of loading at  $\text{pH}_{\text{initial}}$  near neutral.

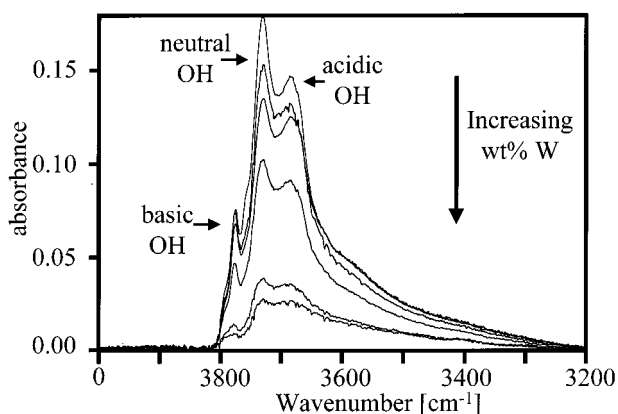


**Figure 8.** IR spectra of tungstate/ $\text{Al}_2\text{O}_3$  as a function of loading at  $\text{pH}_{\text{initial}}$  near neutral.

the CUS sites, partly eliminating them.<sup>12</sup> Consequently, on the  $\text{MoO}_2(\text{acac})_2$  modified  $\text{Al}_2\text{O}_3$  only neutral and acidic OH groups remain. It can be seen in Table 2 that although basic OH groups and CUS sites are not available, a considerable amount of tungstate is adsorbed. Therefore, apparently basic OH groups and CUS sites do not play a role in tungstate adsorption.

An adsorption experiment using  $\text{TiO}_2$  confirmed that tungstate does not adsorb on CUS sites. It was shown<sup>10</sup> that from the 4 wt % Mo present in  $\text{Mo}/\text{TiO}_2$  after AHM adsorption only 0.7 wt % adsorbs on the basic OH groups and the remaining part on CUS sites. Thus, AHM adsorption on  $\text{TiO}_2$  occurs mainly on CUS sites. The AMT adsorption isotherms on  $\text{TiO}_2$  are shown in Figure 9. At near neutral pH, only a small amount of tungstate adsorbs, whereas after decreasing the pH to 1.9, the tungstate adsorption greatly increases. As can be seen in Figure 3, the amount of adsorbed  $\text{NO}_3^-$  on  $\text{TiO}_2$  also increases at lower pH. This means that electrostatic adsorption starts to play a role at lower pH. So, by protonating the basic, neutral, and acidic

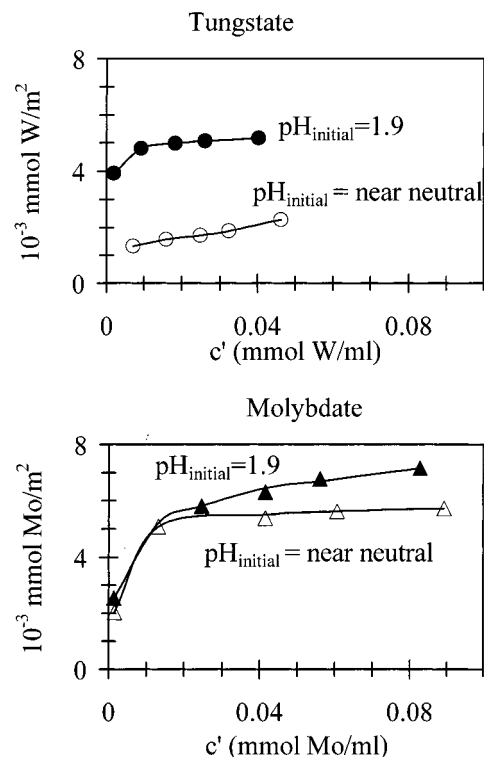


**Figure 9.** Tungstate/ $\text{TiO}_2$  and molybdate/ $\text{TiO}_2$  adsorption isotherms at  $\text{pH}_{\text{initial}}$  near neutral and  $\text{pH}_{\text{initial}}$  1.9.

**TABLE 2. Tungstate and Molybdate Adsorption on  $\text{MoO}_2(\text{acac})_2$  Modified  $\text{Al}_2\text{O}_3$**

sample	preparation	Mo loading $10^{-3}$ mmol/ $\text{m}^2$	W loading $10^{-3}$ mmol/ $\text{m}^2$
A	$\text{MoO}_2(\text{acac})_2$ adsorption	2.1	
B	A + molybdate adsorption	3.1	
C	A + tungstate adsorption	1.8	2.5

OH groups the tungstate adsorption increases, indicating that these groups are more favorable for tungstate adsorption than CUS sites.

In Summary, the tungstate adsorption can be well described by a mechanism of electrostatic reversible adsorption on protonated OH groups especially at lower pH and irreversible reaction with the neutral and acidic OH groups as suggested by the group of Lycourghiotis.<sup>3,5</sup> This tungstate adsorption mechanism is rather different from the adsorption mechanism for molybdate as suggested by van Veen et al.<sup>9-11</sup> They suggested that basic OH groups and CUS sites play an important role in molybdate adsorption.

To check whether tungstate and molybdate adsorb via the same mechanism (as assumed by Lycourghiotis and co-workers<sup>3,5</sup>), the above series of experiments was repeated for molybdate adsorption. The results reveal several differences between adsorption behavior of tungstate and molybdate. (I) Going from near neutral pH to pH 1.9, the amount of adsorbed tungstate increases over the whole W concentration range, whereas the amount of adsorbed molybdate only increases at low Mo concentrations and slightly decreases at higher Mo concentrations (Figure 2). So, Molybdate adsorption only slightly depends on the quantity of protonated OH groups (and so on the pH), whereas tungstate and nitrate adsorption strongly depends on the pH. Previously, we reported,<sup>9</sup> like Wang and Hall,<sup>26</sup> among others, that molybdate adsorption did increase somewhat upon lowering the pH. Nevertheless, we still argued that the modest increase in adsorption capacity indicates that



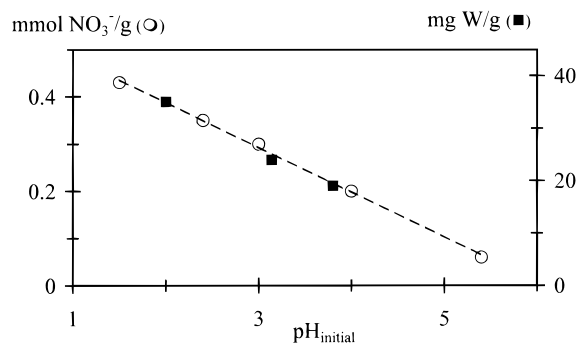


**Figure 10.**  $\text{NO}_3^-/\text{TiO}_2$  and tungstate/ $\text{TiO}_2$  adsorption as a function of  $\text{pH}_{\text{initial}}$ .

surface-charge compensation does not play a major role. We will come back to this point. **(II)** The molybdate uptake is independent of the  $\text{NO}_3^-$  uptake, whereas the tungstate uptake increases with increasing  $\text{NO}_3^-$  uptake (Figure 4). It is clear, especially in the case of  $\text{TiO}_2$ , that tungstate and  $\text{NO}_3^-$  adsorption develop very much the same way with varying  $\text{pH}_{\text{initial}}$  values (Figure 10), whereas molybdate adsorption is hardly affected by it, as can be concluded from the data presented in Figure 9.

This suggests that tungstate adsorbs on the same sites as  $\text{NO}_3^-$ , whereas molybdate does not behave in a like manner. That is, tungstate adsorbs electrostatically on the protonated OH groups, and molybdate does not need these groups for adsorption. **(III)** Much more extra tungstate ( $2.5 \cdot 10^{-3} \text{ mmol/m}^2$ ) than molybdate ( $1.0 \cdot 10^{-3} \text{ mmol/m}^2$ ) adsorbs on  $\text{Al}_2\text{O}_3$  modified with  $\text{MoO}_2(\text{acac})_2$  (Table 2). Because such modified  $\text{Al}_2\text{O}_3$  contains little CUS and basic OH groups, this implies that tungstate, in contrast to molybdate, does not need these groups to adsorb. **(IV)** Van Veen et al.<sup>9</sup> and Sarrazin et al.<sup>13</sup> concluded from IR spectroscopy on  $\text{Al}_2\text{O}_3$  that for molybdate adsorption, the basic OH groups are used first. In the present study, it is found for tungstate adsorption on  $\text{Al}_2\text{O}_3$  that first the neutral and acidic OH groups are involved (Figure 8). **(V)** Much more molybdate adsorbs on  $\text{TiO}_2$  under near-neutral conditions than is the case with tungstate (Figure 9). So, molybdate should be considered to adsorb on CUS sites because a considerable amount of these sites is present on  $\text{TiO}_2$ .<sup>10</sup> Tungstate on the other hand, appears to prefer (protonated) OH sites (see point II). **(VI)** The part of tungstate that can be exchanged for  $\text{SO}_4^{2-}$  is independent of the initial pH, whereas this was not the case for molybdate on  $\text{Al}_2\text{O}_3$  (Figure 6). Molybdate/ $\text{Al}_2\text{O}_3$  prepared at near neutral conditions contains less molybdate exchangeable for  $\text{SO}_4^{2-}$  than Molybdate/ $\text{Al}_2\text{O}_3$  prepared at pH 1.9. This suggests that the fraction of molybdate that adsorbs reversibly increases with decreasing pH. This is indeed in contrast with the conclusion of van Veen et al.<sup>9</sup> that at both pH values the molybdate adsorption sites are the same. However, this conclusion was based on TPR results obtained for Molybdate/ $\text{Al}_2\text{O}_3$  catalysts calcined at 773 K. In view of the known spreading of Mo oxides over the  $\text{Al}_2\text{O}_3$  surface,<sup>27–29</sup> it is reasonable to assume that at high temperature the reversibly adsorbed polymeric molybdates react with the nonbasic OH groups to form irreversibly adsorbed molybdate species.

The foregoing clearly shows that in contrast to the proposition made by Karakostas et al.<sup>5</sup> and Mulcahy et al.<sup>6</sup> tungstate and molybdate adsorb differently. However, the model proposed by van Veen et al.,<sup>9</sup> that molybdate adsorbs on CUS sites, that it reacts with basic OH groups, and that no electrostatically adsorption is involved, is also insufficient to explain all of the present findings. A better description of tungstate and molybdate

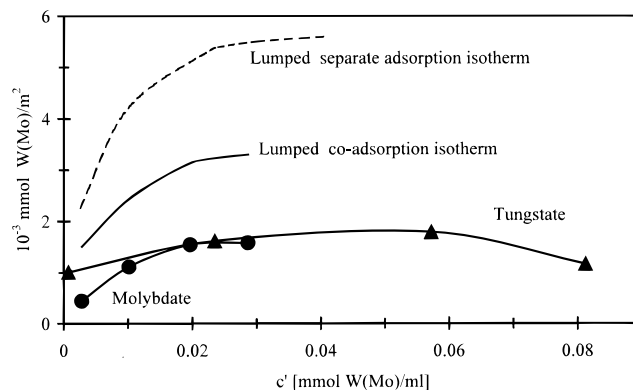


**Figure 11.** Tungstate/ $\text{Al}_2\text{O}_3$  and molybdate/ $\text{Al}_2\text{O}_3$  coadsorption isotherms at  $\text{pH}_{\text{initial}}$  near neutral.

adsorption seems to be a combination of these two propositions. That is, tungstate adsorbs reversibly by electrostatic interactions ( $\text{NO}_3^-$  adsorption parallel, Figure 4) and irreversibly via a reaction with neutral/acidic OH groups (IR spectra, Figure 8). Molybdate adsorbs irreversibly on the basic OH groups, but when these groups are protonated molybdate can also reversibly adsorb via electrostatic interactions.

The results of coadsorption experiments (tungstate and molybdate together in one solution), which were carried out to study whether tungstate and molybdate hinder each other, are in agreement with this model. If tungstate and molybdate compete for the same adsorption sites the sum of tungstate and molybdate adsorbed during coadsorption will be equal to the amount of tungstate *or* molybdate adsorbed separately. On the other hand, if tungstate and molybdate adsorb on different sites, they will not hinder each other, and the sum of tungstate *and* molybdate adsorbed during coadsorption will be equal to the sum of tungstate and molybdate separately.

The equilibrium coadsorption isotherms show (Figure 11) that during this coadsorption mode in total (sum of tungstate *and* molybdate), more metal adsorbs than during separate adsorption (Figure 2). However, the isotherm obtained by lumping coadsorption isotherms lies clearly below the one obtained by lumping the separate adsorption isotherms (Figure 11). This can be explained by assuming that tungstate and molybdate partially have their own preferential adsorption sites and partially compete for the same sites.

Surprisingly, the tungstate coadsorption isotherm under near neutral conditions does not level off at higher concentration but decreases. Possibly, this can be explained by the reversible electrostatic tungstate adsorption and the irreversible molybdate reaction under near neutral conditions. If the surface coverage is so high that steric hindrance plays a role, the reversibly adsorbed tungstate species will be easily removed.

Even more pronounced than in the coadsorption experiment on  $\text{Al}_2\text{O}_3$ , the coadsorption on  $\text{TiO}_2$  shows (Figure 12) that tungstate and molybdate have partially their own adsorption sites and partially compete for the same adsorption sites. As can be seen from Figures 9 and 12, the molybdate adsorption is not affected by the presence of tungstate, but the tungstate adsorption strongly decreases by the presence of molybdate.

Adsorption measurements of tungstate and molybdate were also carried out on amorphous silica alumina (ASA). At the surface of amorphous silica alumina (ASA), different areas can be found, viz. typical  $\text{Al}_2\text{O}_3$  or silica-alumina areas. The sample used for adsorption measurements consisted of 17 wt %  $\text{Al}_2\text{O}_3$  and 83 wt %  $\text{SiO}_2$  that can be considered as pure ASA with little free  $\text{Al}_2\text{O}_3$ . The adsorption isotherms of AHM and AMT

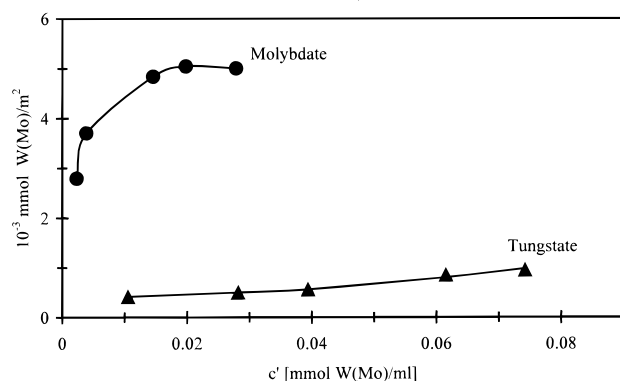


**Figure 12.** Tungstate/TiO<sub>2</sub> and molybdate/TiO<sub>2</sub> coadsorption isotherms at pH<sub>initial</sub> near neutral.

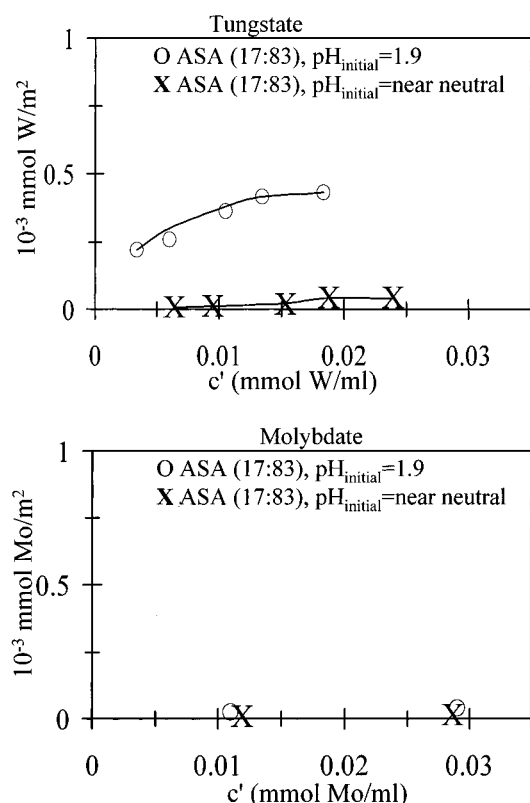


**Figure 13.** Tungstate/ASA and molybdate/ASA adsorption isotherms at pH<sub>initial</sub> near neutral and pH<sub>initial</sub> 1.9.

at near neutral pH and pH 1.9 are shown in Figure 13. On ASA, almost no tungstate and molybdate adsorb at near neutral pH. However, the adsorption of tungstate increases with decreasing pH, whereas that of molybdate remains very small. Therefore, ASA tungstate and molybdate also show a different adsorption behavior. This may indicate that on a composite ASA (containing both alumina and silica alumina areas) molybdate preferentially adsorbs on the alumina areas, whereas tungstate adsorbs at low pH on both type of areas. Preliminary TEM/EDX results pertaining to adsorption on such an ASA (containing 60 wt % Al<sub>2</sub>O<sub>3</sub> and 40 wt % SiO<sub>2</sub>) show that this is indeed the case. In the Mo case, all of it is found on the alumina, whereas the W concentration on the ASA and alumina parts were found to be 1:2. Besides, on SiO<sub>2</sub>, no tungstate or molybdate adsorption on pH<sub>initial</sub> near neutral or pH<sub>initial</sub> 1.9 is observed.

## Conclusion

Tungstate and molybdate are found to adsorb differently. Tungstate adsorbs reversibly by electrostatic interaction with

protonated OH groups and irreversibly by reaction with the neutral and acidic OH groups. Molybdate adsorbs on the coordinatively unsaturated sites and irreversibly in a reaction with the basic OH groups and when these groups are protonated reversibly by electrostatic interaction. These preferences for adsorption sites will be reflected in the way tungstate and molybdate coordinate to the support. As TiO<sub>2</sub> contains mainly CUS sites, there is almost no interaction with tungstate, whereas there is a considerable interaction with molybdate. Also in the case of an ASA support tungstate and molybdate adsorb differently, most likely resulting in a different distribution over the alumina and silica alumina areas.

**Acknowledgment.** These investigations have been supported by The Netherlands Foundation for Chemical Research (SON) with financial aid from The Netherlands Technology Foundation (STW). The research has been performed under the auspices of NIOK, The Netherlands Institute for Catalysis Research, Lab Report TUE-00-6-01. The authors thank Mrs. A.M. Elemans-Mehring for assistance with the AAS measurements.

## References and Notes

- (1) Spanos, N.; Vordonis, L.; Kordulis, Ch.; Lycourghiotis, A. *J. Catal.* **1990**, *124*, 301.
- (2) Spanos, N.; Vordonis, L.; Kordulis, Ch.; Koutsoukos, P. G.; Lycourghiotis, A. *J. Catal.* **1990**, *124*, 315.
- (3) Spanos, N.; Lycourghiotis, A. *J. Catal.* **1994**, *147*, 57.
- (4) Bourikas, K.; Matralis, H. K.; Kordulis, Ch.; Lycourghiotis, A. *J. Phys. Chem.* **1996**, *100*, 11 711.
- (5) Karakostas, L.; Kordulis, Ch.; Lycourghiotis, A. *Langmuir* **1992**, *8*, 1318.
- (6) Mulcahy, F. M.; Fay, M. J.; Proctor, A.; Houalla, M.; Hercules, D. M. *J. Catal.* **1990**, *124*, 231.
- (7) Pizzio, L. R.; Cáceres, C. V.; Blanco, M. N. *Adsorpt. Sci. Technol.* **1991**, *8*, 142.
- (8) Tsigdinos, G. A.; Chen, H. Y.; Streusand, B. J. *Ind. Eng. Chem. Prod. Res. Dev.* **1981**, *20*, 619.
- (9) van Veen, J. A. R.; Hendriks, P. A. J. M.; Romers, E. J. G. M.; Andréa, R. R. *J. Phys. Chem.* **1990**, *94*, 5275.
- (10) van Veen, J. A. R.; de Wit, H.; Emeis, C. A.; Hendriks, P. A. J. M. *J. Catal.* **1987**, *107*, 579.
- (11) van Veen, J. A. R.; Veltmaat, F. T. G.; Jonkers, G. *J. Chem. Soc. Chem. Commun.* **1985**, 1656.
- (12) van Veen, J. A. R.; Jonkers, G.; Hesselink, W. H. *J. Chem. Soc., Faraday Trans. 1* **1989**, *85*, 389.
- (13) Sarrazin, P.; Kasztelan, S.; Payen, E.; Bonnelle, J. P.; Grimblot, J. *J. Phys. Chem.* **1993**, *97*, 5954.
- (14) Pfaff, C.; Pérez Zurita, M. J.; Scott, C.; Patiño, P.; Goldwasser, M. R.; Goldwasser, J.; Mulcahy, F. M.; Houalla, M.; Hercules, D. M. *Catal. Lett.* **1997**, *49*, 13.
- (15) Soung Kim, D.; Wachs, I. E.; Segawa, K. *J. Catal.* **1994**, *146*, 268.
- (16) Kittnell, J. R. USP 3536605, 1968.
- (17) Carier, X.; Lambert, J. F.; Che, M. *J. Am. Chem. Soc.* **1997**, *119*, 10 137.
- (18) Carier, X.; Lambert, J. F.; Che, M. *Stud. Surf. Sci. Catal.* **1998**, *118*, 469.
- (19) Regalbuto, J. R.; Navada, A.; Shadid, S.; Bricker, M. L.; Chen, Q. *J. Catal.* **1999**, *184*, 335.
- (20) Knözinger, H.; Ratnasamy, P. *Catal. Rev. Sci. Eng.* **1978**, *17*, 31.
- (21) Tsyganenko, A. A.; Mardilovich, P. P. *J. Chem. Soc., Faraday Trans.* **1996**, *92*, 4843.
- (22) Schwarz, J. A.; Contescu, C.; Jagiello, J. *Specialist Periodical Reports: Catalysis [Royal Soc. Chem] vol 11*, **1994**, chapter 4.
- (23) Soung Kim, D.; Ostromecki, M.; Wachs, I. E. *J. Mol. Catal. A* **1996**, *106*, 93.
- (24) Vuurman, M. A.; Wachs, I. E. *J. Phys. Chem.* **1992**, *96*, 5008.
- (25) Chan, S. S.; Wachs, I. E.; Murell, L. L. *J. Catal.* **1984**, *90*, 150.
- (26) Wang, L.; Hall, W. K. *J. Catal.* **1982**, *77*, 232.
- (27) Leyrer, J.; Zaki, M. I.; Knözinger, H. *J. Phys. Chem.* **1986**, *90*, 4775.
- (28) Stampfl, S. R.; Chen, Y.; Dumesic, J. A.; Niu, C.; Hill, C. G. *J. Catal.* **1987**, *105*, 445.
- (29) Margraf, R.; Leyrer, J.; Knözinger, H.; Taglauer, E. *Surf. Sci.* **1987**, *189*, 842.